Faithful Fabrication of Biocompatible Multicompartmental Memomicrospheres for Digitally Color-Tunable Barcoding

Guosheng Tang, Long Chen, Zixuan Wang, Shuting Gao, Qingli Qu, Ranhua Xiong, Kevin Braeckmans, Stefaan C. De Smedt, Yu Shrike Zhang,* and Chaobo Huang*

Barcodes have attracted widespread attention, especially for the multiplexed bioassays and anti-counterfeiting used toward medical and biomedical applications. An enabling gas-shearing approach is presented for generating 10-faced microspherical barcodes with precise control over the properties of each compartment. As such, the color of each compartment could be programmatically adjusted in the 10-faced memomicrospheres by using pregel solutions containing different combinations of fluorescent nanoparticles. During the process, three primary colors (red, green, and blue) are adopted to obtain up to seven merged fluorescent colors for constituting a large amount of coding as well as a magnetic compartment, capable of effective and robust high-throughput information-storage. More importantly, by using the biocompatible sodium alginate to construct the multicolor microspherical barcodes, the proposed technology is likely to advance the fields of food and pharmaceutics anti-counterfeiting. These remarkable properties point to the potential value of gas-shearing in engineering microspherical barcodes for biomedical applications in the future.

1. Introduction

Recent advancements in barcodes have brought substantial progresses in various areas, such as anti-counterfeiting,[1] high-throughput bioassays,[2] and information coding.[3] To

G. Tang, L. Chen, S. Gao, Q. Qu, Prof. S. C. De Smedt, Prof. C. Huang
Joint Laboratory of Advanced Biomedical Technology (NFU-UGent)
College of Chemical Engineering
Nanjing Forestry University (NFU)
Nanjing 210037, P. R. China
E-mail: huangchaobo@njfu.edu.cn
G. Tang, Z. Wang, Prof. Y. S. Zhang
Division of Engineering in Medicine
Department of Medicine
Brigham and Women's Hospital
Harvard Medical School
Cambridge, MA 02139, USA
E-mail: yszhang@research.bwh.harvard.edu
Dr. R. Xiong, Prof. K. Braeckmans, Prof. S. C. De Smedt
Laboratory of General Biochemistry and Physical Pharmacy
Faculty of Pharmaceutical Sciences
Ghent University
Ottergemsesteenweg, 460, Ghent 9000, Belgium

The ORCID identification number(s) for the author(s) of this article can be found under https://doi.org/10.1002/smll.201907586.

date, several strategies have been developed and optimized for the fabrication of encoding particles or fibers,[4] including the photobleaching technology,[1a,b,5] as well as photonic,[6] electrical,[7] biomolecular,[8] and microfluidics[9] strategies, among others. Some biomolecular strategies are also demonstrated to be applicable for barcoding.[10] For instance, DNA barcodes are used for rapid, whole genome, single-molecule analyses.[11] Since anti-counterfeiting capacity is indispensable in a number of applications, barcodes have received extensive attention for the purpose. In particular, counterfeit drugs pose a threat to the public health in both developing and industrialized countries because of the high risks and negative outcomes of patients taking or receiving inferior drugs.[12]
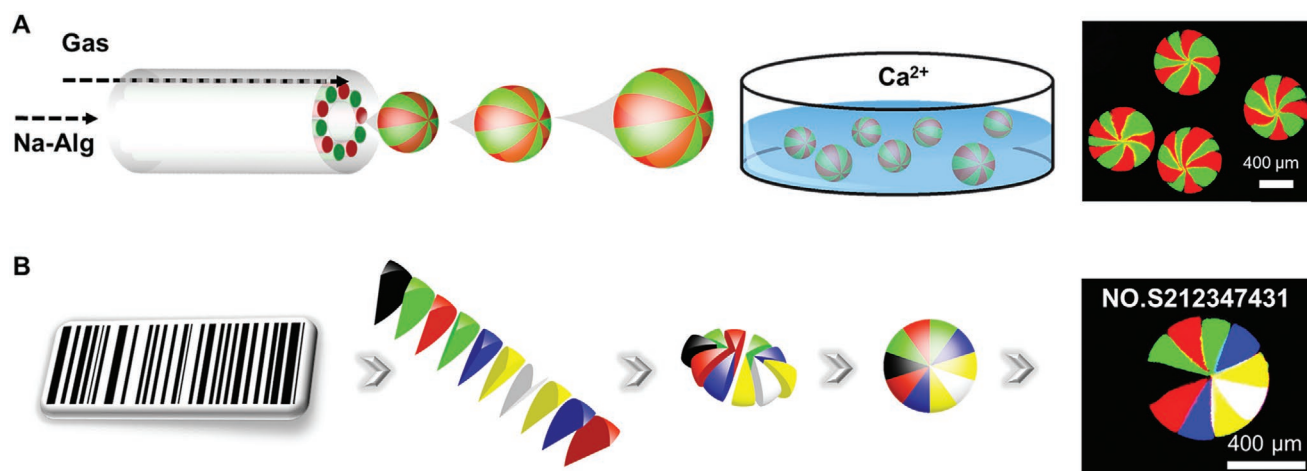
To this end, researchers have exploited considerable strategies for fabricating anti-counterfeiting materials in recent years,[13] in which physical unclonable functions (PUFs) generated through chemical methods, namely, incorporating anti-counterfeiting tags with PUFs, appears to be a potentially enabling strategy.[14] However, most barcodes or anti-counterfeiting methods would inevitably use chemical photoinitiators, crosslinkers, surfactants, and/or United States Food and Drug Administration (FDA)-unapproved polymers, which are unfavorable in the presence of sensitive biomolecules or cells.[13b,15] As such, they are less suitable for applications in drug and food labeling. Until now, the incorporation of barcodes into pharmaceutical preparations remains to be explored as toxicological screening of the coding materials and formulation compatibility testing are required. To expand the range of applications for barcodes, the entire process must remain harmless, and ideally through a time-saving, labor-saving, as well as cost-effective biofriendly technique.

Herein, we report the development of a high-throughput single-step strategy to conveniently produce 10-faced microspherical barcodes by gas-shearing using a custom-designed coaxial nozzle system (**Figure 1**). In the process of preparing the microspheres, programmatically adjusting the different fluorescent nanoparticles in the perfusion channel in the Spray Ejector Device (SED) allowed precise adjustment of the color of each compartment of a microsphere. Besides, we demonstrated that it was feasible to employ only the red, green, and blue fluorescent nanoparticles to build up to 7 colors for barcoding. As such,

ADVANCED
SCIENCE NEWS
www.advancedsciencenews.com

NANO · MICRO
small
www.small-journal.com

Figure 1. Schematics showing the preparation of 10-faced A) multicompartmental microspheres and B) memomicrospheres (i.e., one compartment contains magnetic nanoparticles) to store information.

the resulting microspherical barcodes could be made available in a variety of colors and the use of large amounts of codes for high-throughput anti-counterfeiting applications both in liquid and tablet drugs was possible. This capacity was further added through the utilization of FDA-approved sodium alginate (Na-Alg) to fabricate these microspherical barcodes. More interestingly, via integration of magnetic-responsive Fe_3O_4 nanoparticles into one compartment of the 10-faced microspheres, or so-called memomicrospheres, they were imparted with an orientation behavior under an external magnetic field. As such, we were able to read out the embedded information from the microspherical barcodes in the correct orders. We foresee widespread applications of these biocompatible microspherical barcodes in the areas of food and pharmaceutics anti-counterfeiting.

2. Result and Discussion

The device for continuous generation of 10-faced microspheres included four major components (Figure S1 and Movie S1, Supporting Information): a syringe pump, a collecting bath, a gasholder, and a custom-made coaxial nozzle system termed the SED. As shown schematically in Figure S1A (Supporting Information), the SED was coupled to a syringe loaded with the Na-Alg solution containing different fluorescent polystyrene nanoparticles (200 nm in diameter). In a typical process, gas pulls the growing droplets into the $CaCl_2$ aqueous solution when the shear force is greater than the surface tension (Movie S2, Supporting Information). Then, the $CaCl_2$ aqueous solution in the collection bath crosslinks the droplets into Ca-Alg microspheres (Movie S3, Supporting Information). To compare with our recent work,[16] as also schemed in **Figure 2**A, we first fabricated 8-faced microspheres to evaluate the feasibility of this method. As shown in Figure 2B, 8-faced microspheres were facilely generated. By increasing the number of the needles for the inner flows to 10 (SED-10), as shown in Figure 2C, it was further possible to fabricate 10-faced microspheres with a low polydispersity (Figure 2D), where the size of microspheres could be readily controlled by adjusting the airflow (Figure 2E).

To illustrate the high controllability of each compartment of the microspheres, we adjusted the colors in the specific compartments. As shown schematically in **Figure 3**A,B, we injected Na-Alg solution containing 0.01% red or green fluorescent nanoparticles into the different channels of the SEDs. Revealed experimentally in Figure 3C, up to 9 types of anisotropic microspheres were fabricated via switching the infusion channels of the SEDs, indicating that the pattern of the microspheres was highly controllable.

To further introduce the concept of microspherical barcodes important for the application demonstrated in this work, 0.01% red and green fluorescent nanoparticles were adopted to fabricate 10-faced microspheres of different compartmentalizations. Meanwhile, Fe_3O_4 nanoparticles were introduced as the marker of the barcode reading starting point. As shown in **Figure 4**A, using the SED-10 device, we acquired 10-faced coded memomicrospheres. With the dark compartment as the starting point, the code could be successfully read clockwise (Figure 4B), which indicated the good coding capability of our microspherical barcodes and accurate reading through the embedded magnetic compartment to achieve precise positioning. Two examples of other sets of microspherical barcodes are shown in Figure 4C.

Finally, we employed the red, green, and blue fluorescent nanoparticles to fabricate 10-faced microspheres for generating a considerable number of fluorescent barcodes of various color combinations. We first fabricated the isotropic microspheres (**Figure 5**A-i). Based on red, green, and blue fluorescence, there were altogether 7 colors attainable through different combinations of the fluorescent nanoparticles according to the mixing rule of the three primary colors (Figure 5A-ii). As such, the prepared microspheres containing different fluorescent nanoparticles in the different compartments could be mixed and superimposed to obtain the spectrum of 7 fluorescent colors, i.e., red, green, blue, yellow, magenta, cyan, and white (experimentally shown in Figure 5A-iii,-iv). Based on this premise, 10-faced fluorescent memomicrospheres with a different color in each compartment plus a magnetic compartment were successfully fabricated (Figure 5B-i). Subsequently, the coding information was obtained by decoding the memomicrospheres
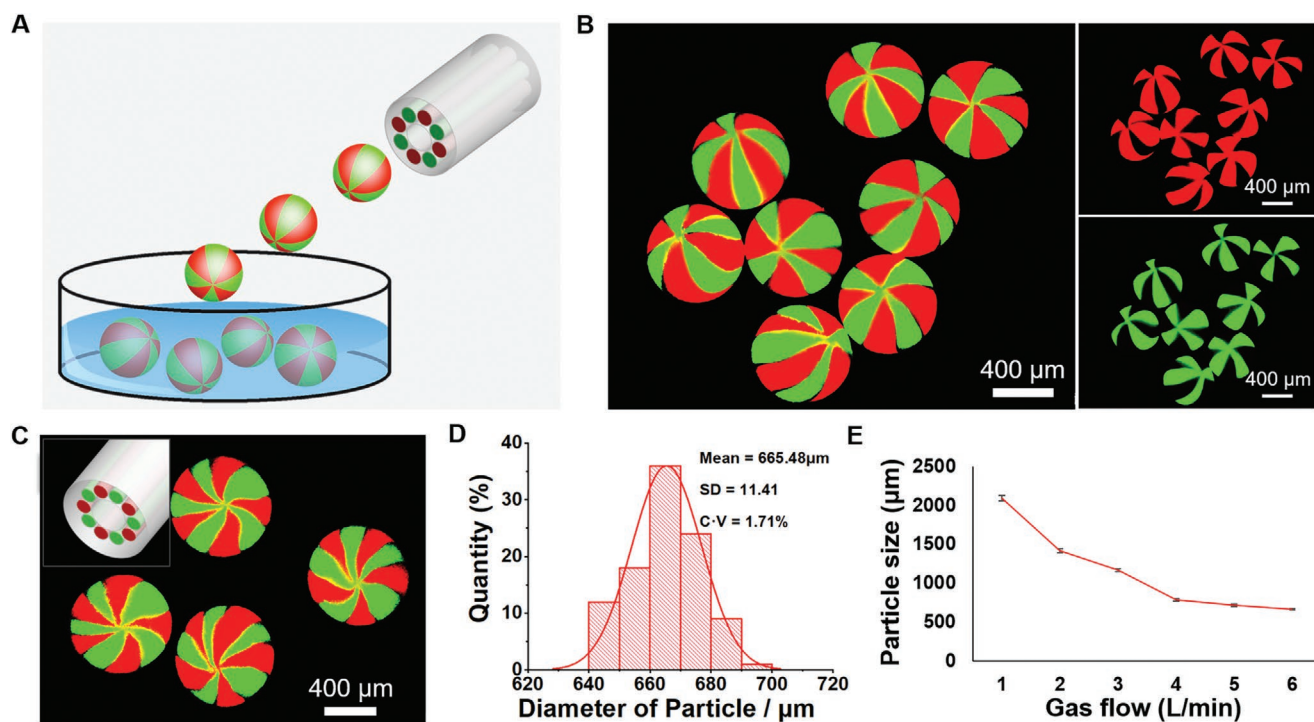
Figure 2. The generation of the 8- and 10-faced microspheres. A) Schematic illustration of an SED for generating anisotropic microspheres. B,C) Fluorescence images of the obtained (B) 8- and (C) 10-faced microspheres and loaded with green or red polystyrene nanospheres (200 nm) in different compartments, produced by gas-shearing of Na-Alg. D) The size distribution of the 10-faced microspheres. E) The relationship between the size of the 10-faced microspheres and the gas flow.
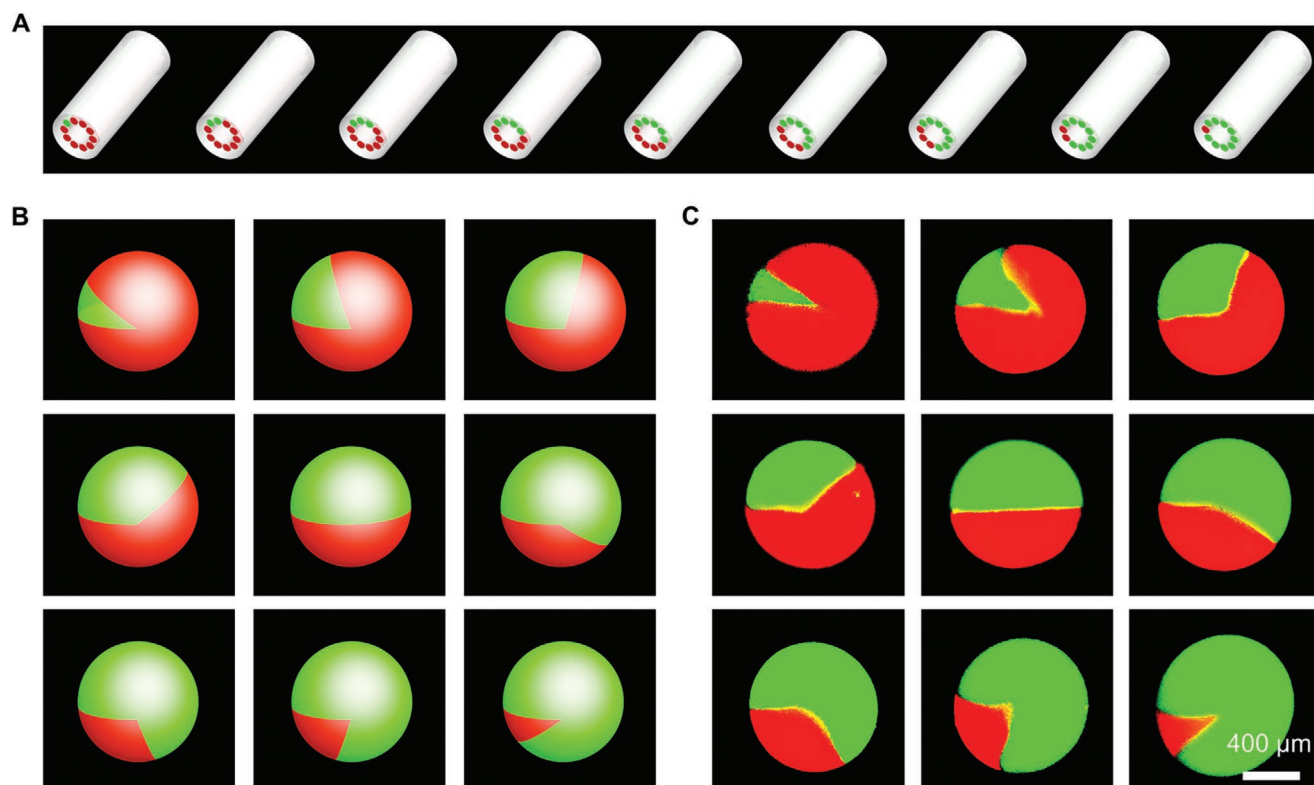
Figure 3. The controllable encoding design of the multicompartmental microspheres fabricated from gas-shearing. A,B) Schematic illustrations of the different SEDs and the corresponding fabricated microspheres. C) Fluorescence images of experimentally obtained multicompartmental microspheres corresponding to the schematics illustrated in (B).
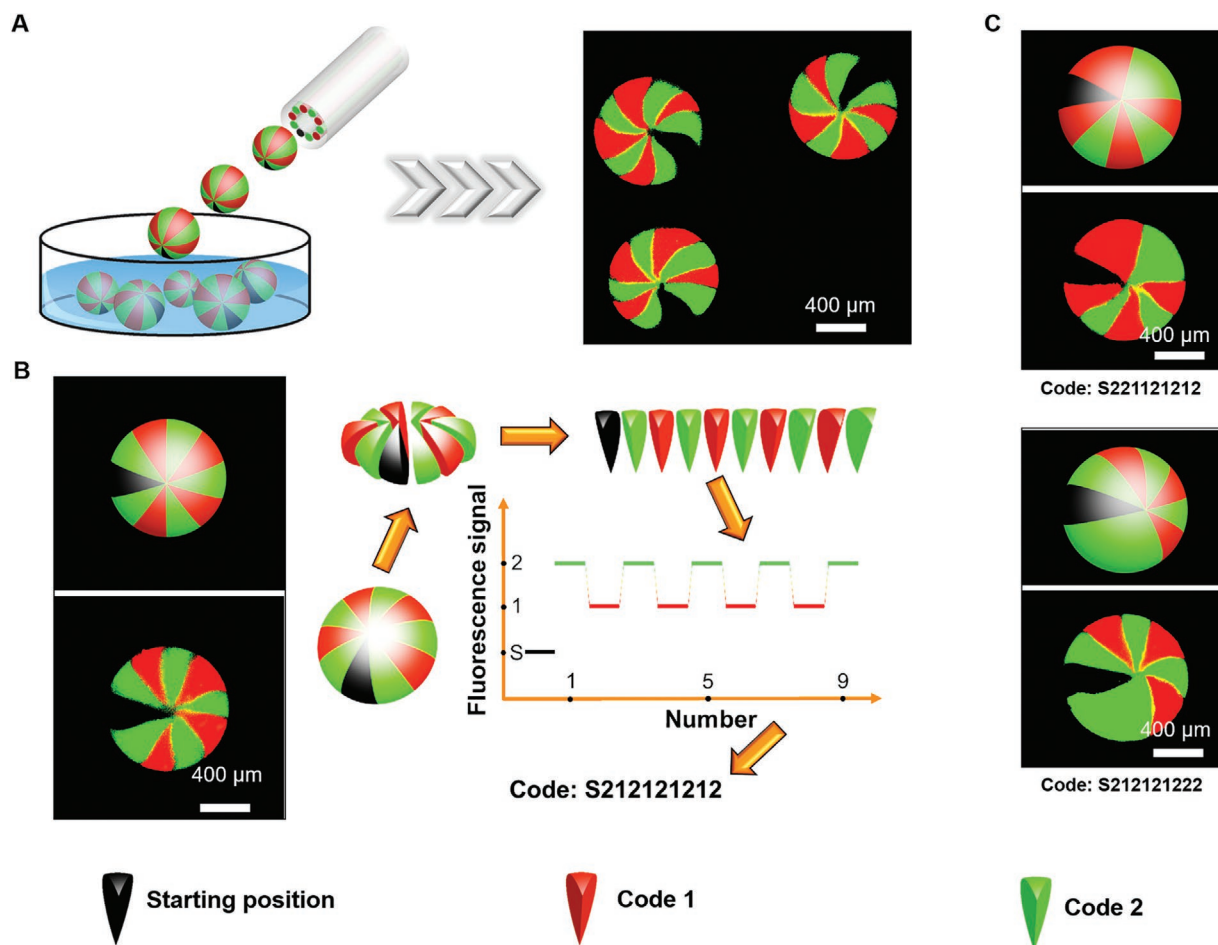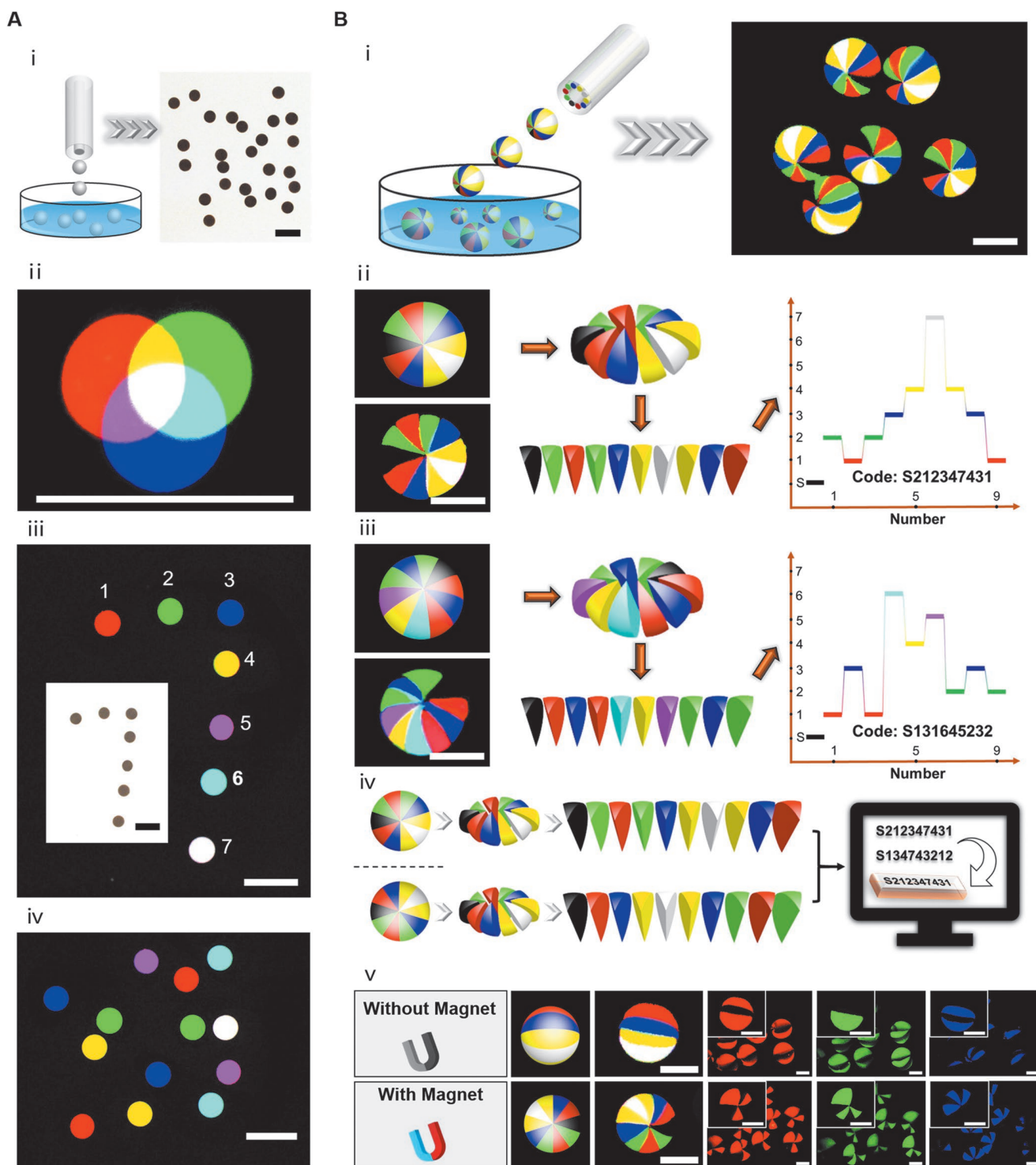
Figure 4. A) Fabrication of memomicrospheres based on red and green colors. B) Process for decoding the memomicrosphere information. C) Two examples of memomicrospheres with different barcoding information.

(Figure 5B-ii,-iii). It is worth noting that, since the microspheres were spherically symmetric, there existed two ways (clockwise and counterclockwise) to read out the coding information from these memomicrospheres, and as such, we defined that both decoding approaches, clockwise and counterclockwise, signified the same set of codes to further improve the barcoding security (Figure 5B-iv). In essence, for information storage and encoding capabilities, taking these 10-faced microspheres as an example, the total number of codes easily exceeds 4 million when 7 colors are used (i.e., 9^7, or 4 782 969 combinations excluding one component used for magnetic nanoparticles).

As above-mentioned, to enhance the controllability of our readout, we incorporated Fe_3O_4 nanoparticles into one compartment of the 10-faced microspheres endowing them with magnetic responsiveness (i.e., the memomicrospheres, Figure S2 and Movie S4, Supporting Information). As indicated in Figure 5B-v, the information was accessible only when the memomicrospheres held the proper orientation under an external magnetic field (Movie S5, Supporting Information). Besides convenient information reading, the magnetic-responsive characteristic of the memomicrospheres enables easy retrieval as well. Of note, magnetic nanoparticles are cost-effective and widely used in the biomedical field,[17] which makes them suitable for our intended application.

Collectively, these features of our microspherical barcodes have undoubtedly offered greater reliability and robustness for their future anti-counterfeiting and information storage applications. In our previous work, although we demonstrated that 8-compartmental microspheres including two fluorescence colors could be fabricated, such microspheres did not show the coding capability that allowed storage of information. This current work has made it possible to establish the concept of microspherical barcodes (memomicrospheres) using the 3 primary colors to build up to 7 fluorescence colors. To our knowledge, the successful fabrication of 10-faced microspherical barcodes with memory capacity has not been reported before. Current technologies are limited to 6-faced microspheres yet without robust coding ability.[18]

To expand our information storage capabilities, we also used the memomicrospheres of different sizes simultaneously. As schemed in Figure S3A (Supporting Information), two sizes of the 10-faced memomicrospheres of different barcoding could be obtained with different airflow rates. The prepared microspherical barcodes and the corresponding decoding information are shown in Figure S3B (Supporting Information). Since a number of memomicrospheres in different sizes may be employed together with these multifaced microspheres

ADVANCED
SCIENCE NEWS
www.advancedsciencenews.com

NANO · MICRO
small
www.small-journal.com

Figure 5. Fabrication of memomicrospheres using only 3 primary colors. A) Construction of standard colors base on 3 primary colors. i) Schematic illustration of an SED-1 for generating isotropic microspheres and the experimentally obtained microspheres. ii) Combination of microspheres with red, green, and blue channels to obtain seven standard colors. iii) Fluorescence image of the obtained seven uniform colors in the microspheres through merging of the 3 primary colors. The inset is the bright-field image corresponding to the fluorescent image. iv) Fluorescence images of a random mixture of differently colored microspheres. B) i) Schematic illustration of the generation process of memomicrospheres and the experimentally obtained superimposed fluorescence image. ii,iii) Decoding process of the obtained two groups of memomicrospheres with different color combinations. iv) The two barcode reading directions for a single memomicrosphere. v) Reading of valid information under external magnetic field guidance. Scale bars: 400 μm.

featuring different compartments, the capacity of information storage of our microspherical barcodes can be greatly expanded beyond through only color combinations.

To demonstrate the reproducibility of the microspherical barcodes, we analyzed the intensity variations of the main colors across multiple memomicrospheres made in a single batch. The results indicated that the intensities of the main colors remained relatively stable as long as we used the same imaging conditions; for red, green, blue, and yellow, the coefficient of variations (CoVs) were found to be 4.61%, 0.85%, 2.25%, and 2.05%, respectively (Table S1, Supporting Information). Such CoVs could have arisen from the slight mixing inhomogeneity when constituting the color solutions, or from the inhomogeneous light illumination in the field of view during imaging. However, this level of variation should still be within the tolerance of our readouts.

Furthermore, to evaluate the real-word application feasibility of our strategy, it is necessary to demonstrate that the fluorescence intensities of these microspherical barcodes could be retained for an extended period of time. Consequently, we observed the fluorescence intensities of our microparticles and found that indeed, the fluorescence intensities of all three primary colors remained largely unchanged for up to 120 days assessed (Figure S4, Supporting Information). However, it is worth noting that our strategy does not necessarily rely on the intensities of the different colors but rather their barcoding information, and therefore, even if the intensities vary across the memomicrospheres or overtime, it would not affect the decoding results.

Our previous work demonstrated that the Na-Alg multifaced microspheres were highly cytocompatible,[12] which are suitable for use in food or pharmaceutical anti-counterfeiting. The microspheres processed 0.01% of fluorescent polystyrene nanoparticles, which was estimated that for the 600 µm memomicrospheres there were merely as little as 0.11 µg of polystyrene in each of them, rendering them essentially harmless considering the bioinertness of the material. Impurities in a drug formulation are deemed acceptable as long as their daily intake remains no more than 1.5 mg.[1b]

To demonstrate the anti-counterfeiting capability of the microspherical barcodes, their potential value in serving as authenticating information was finally illustrated over a range of complex substrates, including both liquid and solid pharmaceutical packaging (**Figure 6**). In the case of anti-counterfeiting for liquid drugs, we were able to add the microtaggants directly into the liquid drugs because of the good biocompatibility of the memomicrospheres. Besides, the size of the memomicrospheres could be controlled to be greater than 300 µm, which is typically larger than most syringe needles used to withdraw liquid drugs, to effectively avoid memomicrospheres from being sucked into the syringes for subsequent patient administration. As shown in Figure 6A, it was easy to read out the coding information with magnetic responsiveness. For solid drug anti-counterfeiting, one capsule on each tablet panel may be used for hosting the memomicrospheres in liquid to achieve the purpose. As revealed in Figure 6B, when the authenticity of the drug needed to be assessed, the tablet could be placed on a microscope stage to read out the coding information with the help of an external magnetic field, which is convenient. We believe that the microspherical barcodes established here might provide an effective strategy to store information or data and help the identification and track-and-trace monitoring of these pharmaceutical products. Besides, attributed to the diversities of the patterns that can be formed within the
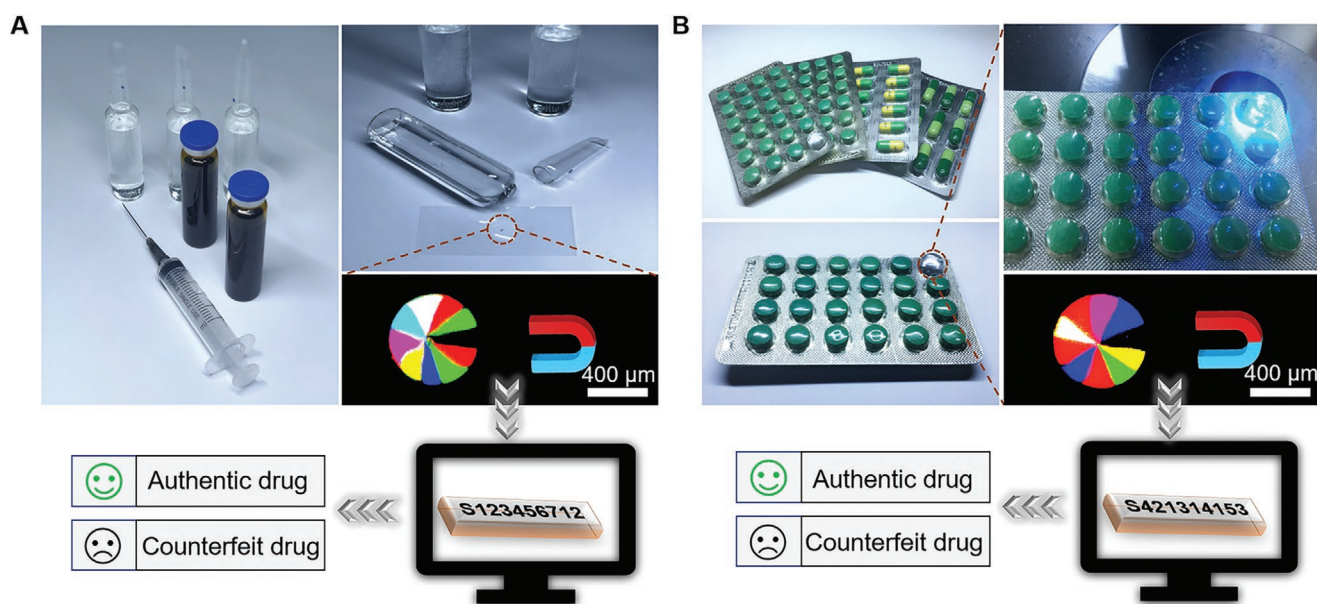
Figure 6. Anti-counterfeiting applications of the memomicrospheres as barcode labels. A) Illustrations of the microspherical barcodes showing coding abilities when directly adding the microtaggants into the liquid preparations and the decoding information using an external magnetic field. B) Illustrations of the microspherical barcodes showing coding abilities when they were used in one capsule on each tablet panel for medicinal tablet packaging and the decoding of the information under a magnet.

memomicrospheres, the amounts of microspherical barcodes are expected to be more than enough for encoding the general manufactured products in daily life.

3. Conclusions

In summary, we have presented the use of a gas-shearing approach for generating the 10-faced memomicrospheres with 7 coding colors by simply merging 3 primary colors in different combinations. The fabrication process was high-throughput (>5000 memomicrospheres per min) and biofriendly, which occurs without the use of organic chemical processes. Na-Alg, an FDA-approved, biocompatible and biodegradable material was used as the primary component of the memomicrospheres. The access of coding information of the resultant microspherical barcodes was facilitated by locking their orientations through magnetic nanoparticle introduction, which further increased information security. Besides, the number of possible barcodes was expected to be large with our 7-color mechanism and fabrication of microspheres with controllable sizes. These results indicated that our microspherical barcodes, or the memomicrospheres, may find widespread applications as convenient and versatile microtaggants for anti-counterfeiting in the food and drug industries in the future.

4. Experimental Section

Materials: Na-Alg was purchased from Sinopharm Chemical Reagent Co., Ltd. (China). Fluoro-Max fluorescent polystyrene nanoparticles R200 (excitation/emission: 542/612 nm), G200 (468/508 nm), and B200 (365/445 nm) were purchased from Thermo Scientific (MA, USA). Fe_3O_4 nanoparticles (30 nm) were purchased from Shanghai Macklin Biochemical Co., Ltd. (China). Float-type flowmeters (LAB-3WB, LZB-6WB) were purchased from Xiangyun Flow Meter Factory (China). Air compressor (Jieba TGY-680-30) was purchased from Shenzhen Yunsite Technology Co., Ltd. (China). All other chemical reagents were of the highest grade available and used as received.

In all experiments, unless otherwise specified, the collecting bath was 2% w/v calcium chloride ($CaCl_2$) aqueous solution, the pregel aqueous phase was 2% w/v Na-Alg aqueous solution with ≈0.01% w/v fluorescent polystyrene nanoparticles, the collector receiving distance was 10 cm, the airflow rate was 6 L min^{-1}, the angle between the smart ejector and collector was 90°, and the flow rate of the Na-Alg was 1 mL h^{-1}. The solutions were all filtered before pumping into the SED. Blunt needles and epoxy adhesive were purchased from Taobao (China).

Equipment: As shown in Figure S1A (Supporting Information), the equipment for fabrication of the microparticles through gas-shearing consists of four major parts: a digital syringe pump (to pump the Na-Alg solution, a collecting bath (2% w/v $CaCl_2$) to gather the microparticles, a gas-holder (which provides the airflow and is controlled by a rotameter), and a custom-made SED (see below). The SED-10 device consisted of a bundle of 10 needles (30G) serving as the core for liquid flows, which was coaxially inserted into a holder needle (22G) as the support. This setup was further inserted into a sheath needle (10G) allowing for the air flow. All the junctions were sealed using epoxy. For SED-8, a bundle of 8 core needles (30G) was inserted into the holder needle (25G) and then into the sheath needle (10G).

Fabrication of Multicompartmental Microspheres by Gas-Shearing: Isotropic microspheres were prepared by processing a Na-Alg solution through an SED-1. The airflow was set at 0.6 L min^{-1}. Eight- and 10-faced microspheres were prepared in a similar way with isotropic microspheres by employing the SED-8 and SED-10, respectively. To visualize the various compartments in the microspheres, red, green, and blue fluorescent polystyrene nanoparticles in different combinations were added to the Na-Alg solutions (the concentration of the polystyrene nanoparticles was ≈0.01% w/v).

Characterizations of the Multicompartmental Microspheres: The production of the 10-faced microdroplets was monitored in real-time using a microscope (C6230, Shanghai Zhong Chen Digital Technic Apparatus, China) and recorded by a high-speed camera (CCD, DH-MER-130-30UM, China Daheng Group, China).

Attainment of Encoded Microspherical Barcode Images: Bright-field and fluorescence images were snapped by optical microscopy (OLYMPUS IX53, Japan). The 3 primary colors including red, green, and blue (R, G, B) of the microspheres were imaged first separately with corresponding excitation lights and filters. Subsequently, the images were superimposed to build a new image containing multiple colors to obtain the microspherical barcodes (Figure S5, Supporting Information).

Supporting Information

Supporting Information is available from the Wiley Online Library or from the author.

Conflict of Interest

The authors declare no conflict of interest.

[1] a) K. Braeckmans, S. C. De Smedt, C. Roelant, M. Leblans, R. Pauwels, J. Demeester, *Nat. Mater.* **2003**, *2*, 169; b) C. Huang, B. Lucas, C. Vervaet, K. Braeckmans, S. Van Calenbergh, I. Karalic, M. Vandewoestyne, D. Deforce, J. Demeester, S. C. De Smedt, *Adv. Mater.* **2010**, *22*, 2657; c) Y. Liu, L. Shang, H. Wang, H. Zhang, M. Zou, Y. Zhao, *Mater. Horiz.* **2018**, *5*, 979; d) H. Tan, G. Gong,

ADVANCED
SCIENCE NEWS

www.advancedsciencenews.com

NANO · MICRO

small

www.small-journal.com

S. Xie, Y. Song, C. Zhang, N. Li, D. Zhang, L. Xu, J. Xu, J. Zheng, *Langmuir* **2019**, *35*, 11503.

[2] a) H. Lee, J. Kim, H. Kim, J. Kim, S. Kwon, *Nat. Mater.* **2010**, *9*, 745; b) Y. Leng, K. Sun, X. Chen, W. Li, *Chem. Soc. Rev.* **2015**, *44*, 5552; c) Y. Zhao, Y. Cheng, L. Shang, J. Wang, Z. Xie, Z. Gu, *Small* **2015**, *11*, 151; d) Y. Xu, H. Wang, B. Chen, H. Liu, Y. Zhao, *Sci. China Mater.* **2019**, *62*, 289; e) M. Yang, Y. Liu, X. Jiang, *Chem. Soc. Rev.* **2019**, *48*, 850.

[3] Q. Y. Yang, M. Pan, S. C. Wei, K. Li, B. B. Du, C. Y. Su, *Inorg. Chem.* **2015**, *54*, 5707.

[4] a) K. Nicolaou, X. Y. Xiao, Z. Parandoosh, A. Senyei, M. P. Nova, *Angew. Chem., Int. Ed. Engl.* **1995**, *34*, 2289; b) Y. Ke, S. Lindsay, Y. Chang, Y. Liu, H. Yan, *Science* **2008**, *319*, 180; c) D. R. Walt, *Chem. Soc. Rev.* **2010**, *39*, 38; d) S. Rauf, A. Glidle, J. M. Cooper, *Adv. Mater.* **2009**, *21*, 4020.

[5] F. Fayazpour, B. Lucas, N. Huyghebaert, K. Braeckmans, S. Derveaux, B. G. Stubbe, J. P. Remon, J. Demeester, C. Vervaet, S. C. De Smedt, *Adv. Mater.* **2007**, *19*, 3854.

[6] a) F. Ramiro-Manzano, R. Fenollosa, E. Xifre-Perez, M. Garin, F. Meseguer, *Adv. Mater.* **2011**, *23*, 3022; b) Y. Qi, W. Niu, S. Zhang, S. Wu, L. Chu, W. Ma, B. Tang, *Adv. Funct. Mater.* **2019**, *29*, 1903743; c) J. Ji, W. Lu, Y. Zhu, H. Jin, Y. Yao, H. Zhang, Y. Zhao, *ACS Sens.* **2019**, *4*, 1384; d) Y. Yao, Z. Gao, Y. Lv, X. Lin, Y. Liu, Y. Du, F. Hu, Y. S. Zhao, *Angew. Chem., Int. Ed.* **2019**, *58*, 13803.

[7] X. Zhang, H. Su, S. Bi, S. Li, S. Zhang, *Biosens. Bioelectron.* **2009**, *24*, 2730.

[8] N. Yu, Y. L. Wei, X. Zhang, N. Zhu, Y. L. Wang, Y. Zhu, H. P. Zhang, F. M. Li, L. Yang, J. Q. Sun, A. D. Sun, *Sci. Rep.* **2017**, *7*, 5037.

[9] C.-G. Yang, L. Cheng, W.-Q. Ye, D.-H. Zheng, Z.-R. Xu, *Colloids Surf. A* **2020**, *588*, 124373.

[10] Gentile, S. D.; Griebel, M. E.; Anderson, E. W.; Underhill, G. H., *Bioconjugate Chem.* **2018**, *29*, 2846.

[11] N. O. Wand, D. A. Smith, A. A. Wilkinson, A. E. Rushton, S. J. W. Busby, I. B. Styles, R. K. Neely, *Nucleic Acids Res.* **2019**, *47*, 68.

[12] a) P. Aldhous, *Nature* **2005**, *434*, 132; b) T. Parfitt, *Lancet* **2006**, *368*, 1481.

[13] a) J. Liao, C. Zhu, C. Bao, Z. Zhao, X. Liu, L. Tian, Y. Zeng, X. Zhou, Z. Xie, Z. Gu, *Adv. Funct. Mater.* **2019**, *29*, 1902954; b) X. Ji, R. T. Wu, L. Long, X. S. Ke, C. Guo, Y. J. Ghang, V. M. Lynch, F. Huang, J. L. Sessler, *Adv. Mater.* **2018**, *30*, 1705480; c) S. Armstrong, *Nat. Photonics* **2012**, *6*, 801; d) I. B. Burgess, M. Lončar, J. Aizenberg, *J. Mater. Chem. C* **2013**, *1*, 6075; e) Z. Li, H. Chen, B. Li, Y. Xie, X. Gong, X. Liu, H. Li, Y. Zhao, *Adv. Sci.* **2019**, *6*, 1901529; f) Y. Zheng, C. Jiang, S. H. Ng, Y. Lu, F. Han, U. Bach, J. J. Gooding, *Adv. Mater.* **2016**, *28*, 2330; g) Y. Liu, F. Han, F. Li, Y. Zhao, M. Chen, Z. Xu, X. Zheng, H. Hu, J. Yao, T. Guo, W. Lin, Y. Zheng, Y. You, P. Liu, Y. Li, L. Qian, *Nat. Commun.* **2019**, *10*, 2409.

[14] a) R. Arppe, T. J. Sørensen, *Nat. Rev. Chem.* **2017**, *1*, 0031; b) S. Shikha, T. Salafi, J. Cheng, Y. Zhang, *Chem. Soc. Rev.* **2017**, *46*, 7054; c) B.-H. Wu, C. Zhang, N. Zheng, L.-W. Wu, Z.-K. Xu, L.-S. Wan, *ACS Appl. Polym. Mater.* **2018**, *1*, 47.

[15] a) Y. Xu, X. Zhang, C. Luan, H. Wang, B. Chen, Y. Zhao, *Biosens. Bioelectron.* **2017**, *87*, 264; b) K. Zhong, J. Li, L. Liu, S. Van Cleuvenbergen, K. Song, K. Clays, *Adv. Mater.* **2018**, *30*, 1707246.

[16] G. Tang, R. Xiong, D. Lv, R. X. Xu, K. Braeckmans, C. Huang, S. C. De Smedt, *Adv. Sci.* **2019**, *6*, 1802342.

[17] J. Kudr, Y. Haddad, L. Richtera, Z. Heger, M. Cernak, V. Adam, O. Zitka, *Nanomaterials* **2017**, *7*, 243.

[18] K. Maeda, H. Onoe, M. Takinoue, S. Takeuchi, *Adv. Mater.* **2012**, *24*, 1304.